

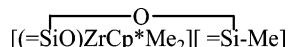
Synthesis, Characterization, and Activity in Ethylene Polymerization of Silica Supported Cationic Cyclopentadienyl Zirconium Complexes

Nicolas Millot, Sophie Soignier, Catherine C. Santini,* Anne Baudouin, and Jean-Marie Basset*

Contribution from the Laboratoire de Chimie Organométallique de Surface, UMR 9986 CNRS - ESCPE Lyon, 43 bd du 11 Novembre 1918, F-69626 Villeurbanne Cedex, France

Received January 19, 2006; E-mail: santini@cpe.fr; basset@cpe.fr

Abstract: Cp*ZrMe₃ reacts with silica pretreated at 800 °C, SiO₂-(800) through two pathways: (a) protolysis of a Zr-Me group by surface silanols and (b) transfer of a methyl group to the surface by opening of strained siloxane bridges, in a relative proportion of ca. 9/1, respectively, affording a well-defined surface species [(≡SiO)ZrCp*(Me)₂], **3**, but with two different local environments **3a**, [(≡SiO)ZrCp*(Me)₂][≡Si-O-Si≡], and the other with **3b**,



The reaction of the species **3** with B(C₆F₅)₃ is controlled by this local environment and gives three surface species [(≡SiO)ZrCp*(Me)]⁺[MeB(C₆F₅)₃]⁻ [≡Si-O-Si≡], **4a** (20%), [(≡SiO)ZrCp*(Me)]⁺[(Me)B(C₆F₅)₃]⁻ [≡Si-Me], **4b** (10%), and [(≡SiO)₂ZrCp*]⁺[(Me)B(C₆F₅)₃]⁻ [≡Si-O-Si≡], **5** (70%). On the contrary, the reaction of Cp*Zr(Me)₃, Cp₂Zr(Me)₂ with [≡SiO-B(C₆F₅)₃][HNEt₂Ph]⁺, **6**, leads to a unique species [(≡SiO)B(C₆F₅)₃]⁻[Cp*Zr(Me)₂·NEt₂Ph]⁺, **7**, and [(≡SiO)ZrCp₂]⁺[(Me)B(C₆F₅)₃]⁻, **9** respectively. The complexes **4** and **7** are active catalysts in ethylene polymerization at room temperature, 93 and 67 kg PE mol Zr¹⁻ atm⁻¹ bar⁻¹, respectively, indicating that covalently bounded Zr catalyst **4** is slightly more active than the “floating” cationic catalyst **7**.

Introduction

In the recent years, one of the most exciting developments in the pluridisciplinary area of catalysis organometallic science has been the new polymerization technologies based on “single-site” metallocene chemistry.^{1,2}

This methodology implies the reaction of a metallocene precursor (typically Cp₂ZrCl₂) with a multifunctional cocatalyst (usually MAO for methylalumoxane). The reaction of the precursor with metallocene is (i) create a metal-alkyl bond necessary for the propagation of the chain in the polymerization process and (ii) create on the metal a cationic charge to render the system more electrophilic and hopefully more active. This last step occurs by removing with a Lewis acid either the remaining anionic chloride or the alkyl resulting from the previous alkylation.^{3,4}

The methodology has been simplified, at least at the university level, by starting with a preformed metal alkyl, in which case the primary role of the cocatalyst would be only that of a Lewis

center with a “noncoordinating” ability once transformed into the corresponding anion. In such, B(C₆F₅)₃ has been found to be an excellent cocatalyst with precursors of the type Cp₂ZrR₂. The active species is a kind of ion pair of the type [Cp₂ZrMe⁺]-[MeB(C₆F₅)₃]⁻.

When applying this methodology to the design of “single site heterogeneous catalysis” based on group 4 complexes attached on a *neutral* surface, such as silica, two different strategies may be used:⁵⁻⁹

(1) graft first a precursor complex directly with the silica surface in order to create a covalently bonded complex of the type [≡SiO-MR_n] followed by the action of an external Lewis co catalyst C leading to the hypothetical **1**: [≡SiO-MR_{n-1}]⁺[CR]⁻

(2) graft first the Lewis acid cocatalyst C directly to the surface in order to create a covalent bond with the surface of the type [≡SiO-C'] and then react this supported Lewis acid cocatalyst with the molecular complex in order to achieve the hypothetical **2** [≡SiO-C'R]⁻[MR_{n-1}]⁺.

If both surface single site complexes could be synthesized and fully characterized, as in **1** and **2**, an interesting question would be to compare the activity of **1** and **2**. Is the presence of the surface ligand, as in **1**, an advantage to achieve the best activity in olefin polymerization?

- (1) Kaminsky, W., Ed. *Metalorganic Catalysts for Synthesis and Polymerisation: Recent Results by Ziegler-Natta and Metallocene Investigations*; Springer-Verlag: Berlin, 1999.
- (2) Chen, E. Y.-X.; Marks, T. J. *Chem. Rev.* **2000**, *100*, 1391–1434.
- (3) Soga, K.; Kaminaka, M. *Makromol. Chem., Macromol. Symp.* **1993**, *194*, 1745–1755.
- (4) Kaminsky, W.; Renner, F. *Makromol. Chem., Rapid Commun.* **1993**, *14*, 239–243.

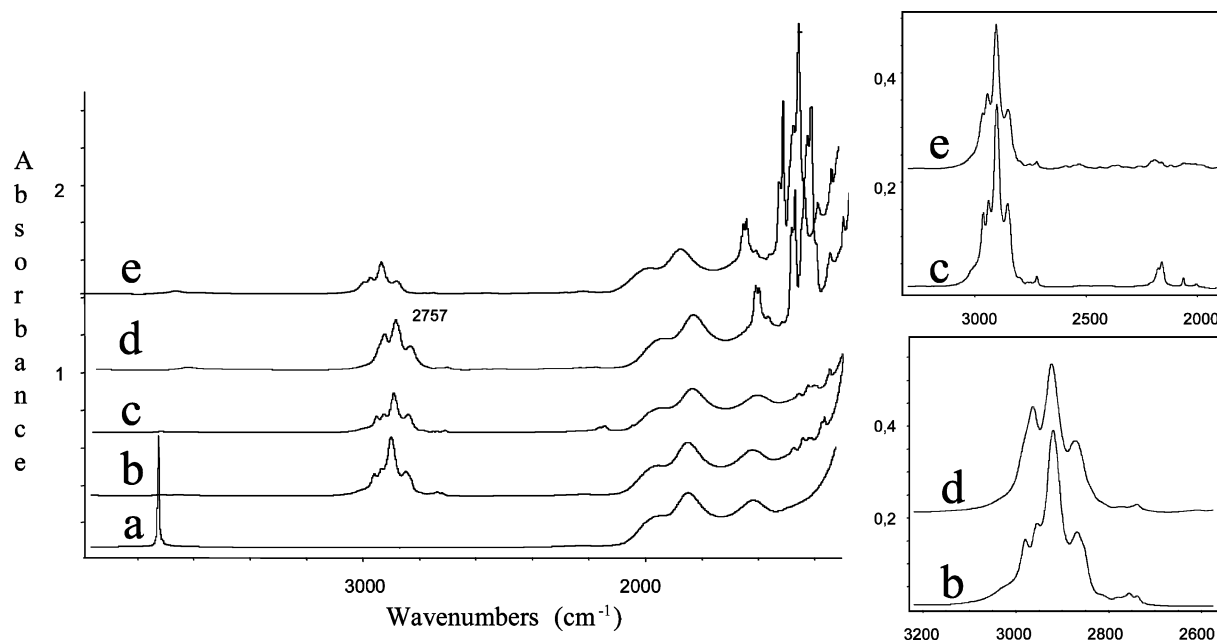


Figure 1. IR spectra of (a) $\text{SiO}_2-(800)$; (b) $\text{SiO}_2-(800) + \text{Cp}^*\text{Zr}(\text{Me})_3$, **3**; (c) $\text{SiO}_2-(800) + \text{Cp}^*\text{Zr}(\text{CD}_3)_3$, **3D**; (d) = (b) + $\text{B}(\text{C}_6\text{F}_5)_3$; (e) = (c) + $\text{B}(\text{C}_6\text{F}_5)_3$.

In this context, we report here the preparation of two series of neutral or cationic surface complexes:

In the first series, as described in **1**, the zirconium is directly linked to the silica surface and the following surface organometallic complexes are $[(\equiv\text{SiO})\text{ZrCp}^*(\text{Me})_2]$, **3**, $[(\equiv\text{SiO})\text{ZrCp}^*(\text{Me})]^+[(\text{Me})\text{B}(\text{C}_6\text{F}_5)_3]^-$, **4**, and the unexpected $[(\equiv\text{SiO})_2\text{ZrCp}^*]^+[(\text{Me})\text{B}(\text{C}_6\text{F}_5)_3]^-$, **5**.

In the second series, various precursors leading to a zirconium “floating” above the silica anionic structure are $[(\equiv\text{SiO})\text{B}(\text{C}_6\text{F}_5)_3][\text{HNEt}_2\text{Ph}]^+$, **6**, $[(\equiv\text{SiO})\text{B}(\text{C}_6\text{F}_5)_3]^-[\text{Cp}^*\text{Zr}(\text{Me})_2\text{NEt}_2\text{Ph}]^+$, **7**, as well as $[(\equiv\text{SiO})\text{ZrCp}_2]^+[(\text{Me})\text{B}(\text{C}_6\text{F}_5)_3]^-$, **9**.

The characterization tools of surface organometallic chemistry are elemental and gas-phase analyses, spectroscopic methods (infrared, multinuclear solid-state NMR), and labeling (^2H , ^{13}C).⁷ Comparative results were achieved by studying catalytic activities of each of these complexes in ethylene polymerization.

Results

I. Reactivity of $\text{Cp}^*\text{Zr}(\text{Me})_3$ with $\text{SiO}_2-(800)$. We have found recently that the reaction of $\text{Cp}^*\text{Zr}(\text{Me})_3$ with partially dehydroxylated silica at 500 °C, afforded mainly $[(\equiv\text{SiO})\text{ZrCp}^*(\text{Me})_2]$, **3**.⁷ However, the close examination of the analytical data indicates that the percentage of zirconium grafted (1.1 Zr/nm²) is lower than the maximum concentration of surface hydroxyl groups (1.4 OH/nm²). This observation along with the fact that all silanols were consumed during grafting means that even if $[(\equiv\text{SiO})\text{ZrCp}^*(\text{Me})_2]$ is the major species obtained via protonolysis of one methyl group by surface silanols (quantitatively evidenced by the evolution of ca. 1.1 equiv of methane),⁷ a secondary reaction could occur with some free surface silanol groups leading to $[(\equiv\text{SiO})_2\text{ZrCp}^*(\text{Me})]$ (up to ca. 10%). In an attempt to avoid this phenomenon which leads to a small

deviation from the “single site” target, we have used a silica surface dehydroxylated at 800 °C ($\text{SiO}_2-(800)$) (containing 0.6 ± 0.1 OH/nm²). The grafting reaction of $\text{Cp}^*\text{Zr}(\text{Me})_3$ with $\text{SiO}_2-(800)$ was performed in the same experimental conditions as those used for $\text{SiO}_2-(500)$ (dry pentane, at room temperature, 3 h).⁷

I.1. Analytical Data on the Grafting. The elemental analysis of the solid samples indicate that the zirconium content (2.22 wt %) corresponding to a surface zirconium concentration (0.81 Zr/nm²) is significantly higher than the silanol concentration (0.6/nm²) (grafted Zr/Si-OH = 1.16). Chemical analysis indicates that 90% of the Zr-Me reacts with the silanols leading to methane and Zr-O-Si (evolution of 0.9 mol of CH₄ per grafted Zr). Since no Cp*H is evolved during the grafting, most of the Cp* are on the surface (most likely linked to Zr). This is confirmed by the elemental analysis (carbon/zirconium molar ratio varying between 12.2 and 12.4.) and the subsequent hydrolysis of the surface, which liberates ca. 2.0 mol of methane per grafted Zr.

These results show that on $\text{SiO}_2-(800)$, as on $\text{SiO}_2-(500)$, one Cp* and two Me groups per zirconium atom are present on the surface likely as $[(\equiv\text{SiO})\text{ZrCp}^*(\text{Me})_2]$. (Note that the mass balance is not perfect for methane 0.9 mol instead of 1 mol and the ratio Zr/SiOH is higher than expected.) The grafting pathway is not only due to a simple protonolysis of Zr-Me by the surface silanols but also probably a quite significant reaction with the strained $[\equiv\text{Si}-\text{O}-\text{Si}\equiv]$ bridges.

I.2. Spectroscopic Data of the Grafting Reaction. The results of infrared spectroscopy are represented in Figure 1a–c. Upon grafting, one observes total disappearance of the $\nu(\text{O}-\text{H})$ band at 3747 cm⁻¹ attributed to isolated silanol groups, Figure 1a and b, and the concomitant emergence of bands at 3100–2700 cm⁻¹ and 1500–1350 cm⁻¹ regions which are ascribed to $\nu(\text{C}-\text{H})$, $\nu(\text{C}=\text{C})$, and $\delta(\text{C}-\text{H})$ vibrations of Cp* and methyl groups.^{7,10,11} Under the same experimental conditions, infrared spectra recorded after reaction of $\text{Cp}^*\text{Zr}(\text{CD}_3)_3$ with pellets of $\text{SiO}_2-(800)$ show $\nu(\text{C}-\text{D})$ and $2\delta(\text{C}-\text{D})$ vibrations

(5) Walzer, J.; Flexer, J. In U.S. Patent 5,643,847; Exxon Chemicals, 1997.

(6) Bochmann, M.; Pindado, G. J.; Lancaster, S. J. *J. Mol. Catal.* **1999**, *144*, 137–150.

(7) Jezequel, M.; Dufaud, V.; Ruiz-Garcia, M. J.; Carrillo-Hermosilla, F.; Neugebauer, U.; Nicolai, G. P.; Lefebvre, F.; Bayard, F.; Corker, J.; Fiddy, S.; Evans, J.; Broyer, J. P.; Malinge, J.; Basset, J.-M. *J. Am. Chem. Soc.* **2001**, *123*, 3520–3540.

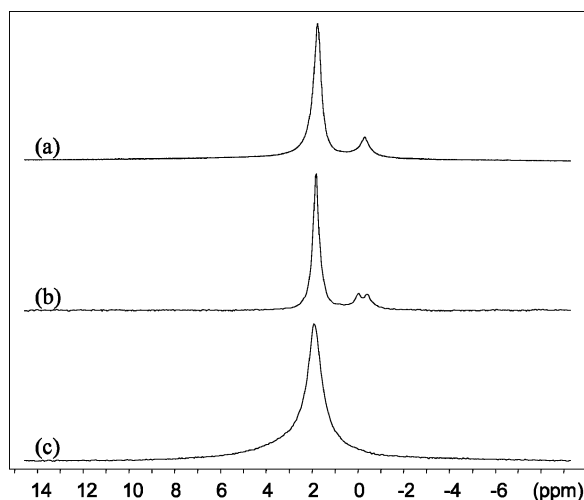


Figure 2. 300 MHz solid state ^1H MAS NMR of (a) **3**, (b) **3***, and (c) **3*** after hydrolysis, spinning speed 10 kHz, recycle delay 2 s.

at 2193, 2175, 2077, and 2021 cm^{-1} consistent with the presence of surface $\text{Zr}-\text{CD}_3$ groups, Figure 1c. Subtraction of the spectra of deuterated surface complexes **3_D** from those of **3** allows us to assign the bands at 2932, 2911, 2852, and 2757 cm^{-1} to, respectively, $\nu_{\text{as}}(\text{C}-\text{H})$, $\nu_{\text{s}}(\text{C}-\text{H})$, and $2\delta_{\text{as}}(\text{C}-\text{H})$ vibrations of the methyl groups bound to the zirconium center. Those at 2980, 2954, 2920, and 2869 cm^{-1} are, respectively, assigned to $\nu_{\text{as}}(\text{C}-\text{H})$, $\nu_{\text{s}}(\text{C}-\text{H})$, and $2\delta_{\text{as}}(\text{C}-\text{H})$ vibrations of the Cp^* methyl groups.

The solid state ^1H NMR spectrum of **3** shows two peaks at 1.7 and -0.25 ppm characteristic, of Me groups on the Cp^* ligand and the zirconium methyl groups, respectively, Figure 2a.^{12–14} Solid state ^{13}C NMR spectra show the presence of three peaks at 121, 38, and 9 ppm attributed to carbons of Cp^* ring and carbons of methyl groups bound to zirconium and Cp^* ligand, respectively, Figure 3a.¹⁴ The ^{13}C labeled surface species $[(\equiv\text{SiO}_{800})\text{ZrCp}^*(^{13}\text{CH}_3)_2]$, **3***, resulting from the reaction of $\text{Cp}^*\text{Zr}(^{13}\text{CH}_3)_3$, with $\text{SiO}_{2-(800)}$, exhibit a doublet at -0.3 ppm ($^1J_{\text{C}-\text{H}} = 112$ Hz) in solid-state ^1H NMR spectra, Figure 2b, and a very intense signal at 39 ppm in solid-state ^{13}C NMR spectra due to the $\text{Zr}-^{13}\text{CH}_3$ groups. It is worth noting that a small signal is observed in ^{13}C NMR spectra at -4.5 ppm, Figure 3b. The intensity of this latter is weak in the spectrum of the labeled species **3*** and is not visible in the spectra of **3**. After hydrolysis of **3***, the peak at 39 ppm, Figure 3c, and the doublet at -0.3 ppm, Figure 2c, respectively, in ^{13}C and ^1H NMR spectra, disappear totally. In ^{13}C NMR spectra, only the

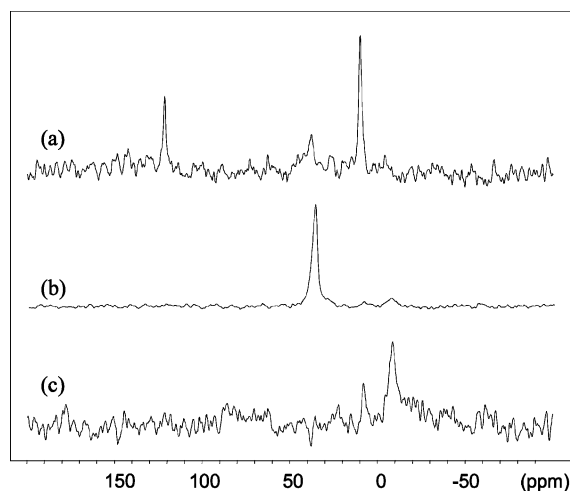


Figure 3. 75 MHz solid state CP-MAS ^{13}C NMR of (a) **3**, (b) **3***, and (c) **3*** after hydrolysis, spinning speed 10 kHz, recycle delay 2 s, contact time 5 ms.

signal due to Cp^* ligand (9 ppm) and the peak at -4.5 ppm are still present, Figure 3c. This latter resonance is unambiguously ascribed to a surface $\equiv\text{Si}-^{13}\text{CH}_3$ moiety which is known to be completely unreactive with water.¹⁵

I.3. Interpretation of the Data. There are several evidences which indicate that Cp^*ZrMe_3 reacts with $\text{SiO}_{2-(800)}$ via two pathways: (a) protolysis of a $\text{Zr}-\text{Me}$ group by surface silanols and (b) transfer of a methyl group to the surface by opening siloxane bridges:

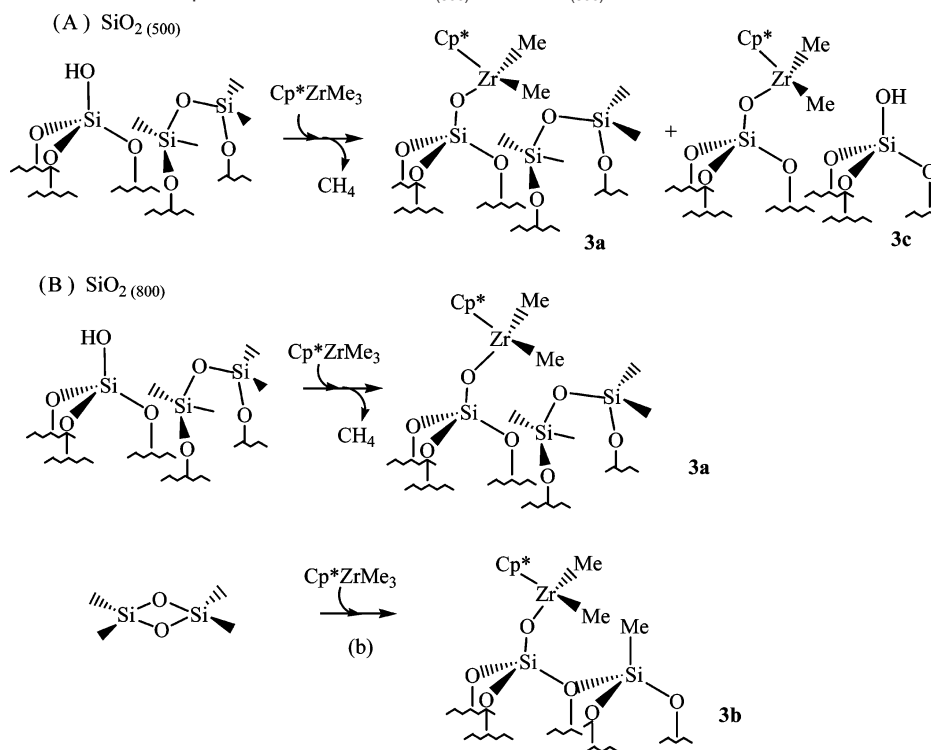
- (i) 0.9 equiv of methane evolved instead of 1 per grafted zirconium,
- (ii) The $\text{Zr}/\text{Si}-\text{OH}$ ratio is higher than 1 for saturated supports (that is supports for which all silanols have been consumed),
- (iii) The presence of surface $\equiv\text{Si}-^{13}\text{CH}_3$ groups evidenced by ^{13}C NMR.

This kind of opening of $[\equiv\text{Si}-\text{O}-\text{Si}\equiv]$ bonds has already been reported. For example alkyl or halogen derivatives of boron,^{16,17} aluminum,¹⁸ and rhenium.¹⁹ An alkyl transfer reaction on a silica surface, evidenced by solid-state ^{13}C NMR spectroscopy, has been reported in the case of thorium and zirconium complexes.^{15,22} This kind of reaction is generally favored with pretreated silica_(500–1200°C). The high dehydroxylation temperature causes the condensation of isolated hydroxyl groups, giving rise to highly strained and reactive $[\equiv\text{Si}-\text{O}-\text{Si}\equiv]$ bridges with a density of 0.1 $[\equiv\text{Si}-\text{O}-\text{Si}\equiv]/\text{nm}^2$ at 800 °C and a maximum of 0.15 $[\equiv\text{Si}-\text{O}-\text{Si}\equiv]/\text{nm}^2$ at 1200 °C.^{18,20,21}

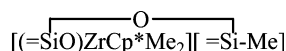
In conclusion, on silica₍₅₀₀₎, one reaches two types of surface sites, one similar to **3** but with two different environments ($\equiv\text{Si}-\text{OH}$ and $[\equiv\text{Si}-\text{O}-\text{Si}\equiv]$) and one with a bipodal zirconium. In contrast, the reaction of Cp^*ZrMe_3 with $\text{SiO}_{2-(800)}$, the two pathways (a) and (b) shown in Scheme 1 are present in a relative proportion of ca. 9/1, respectively, affording a well-defined surface species $[(\equiv\text{SiO})\text{ZrCp}^*(\text{Me})_2]$, **3**, in two different

- (8) Millot, N.; Cox, A.; Santini, C. C.; Mollard, Y.; Basset, J.-M. *Chem.—Eur. J.* **2002**, *8*, 1438 and references therein. (b) Millot, N.; Santini, C. C.; Baudouin, A.; Basset, J.-M. *Chem. Commun.* **2003**, 2034–2035.
- (9) Hlatky, G. G.; Upton, D. J.; Turner, H. W. PCT Int. WO 91/09882, 1991, Exxon Chemical Co. (b) Yang, X.; Stern, C. L.; Marks, T. J. *Organometallics* **1991**, *10*, 840–842. (c) Bochmann, M.; Lancaster, S. J. *J. Organomet. Chem.* **1992**, *434*, C1. (d) Hlatky, G. G.; Eckman, R. R.; Turner, H. W. *Organometallics* **1992**, *11*, 1413–1416.
- (10) Siedle, A. R. *J. Organomet. Chem.* **1995**, *497*, 119.
- (11) (a) McGrady, G. S.; Downs, A. J.; Hamblin, J. M. *Organometallics* **1995**, *14*, 3783–3790. (b) McQuillan, G. P.; McKean, D. C.; Torto, I. J. *Organomet. Chem.* **1986**, *312*, 183–195.
- (12) Wang, Q.; Qouyoum, R.; Gillis, D. J.; Tudoret, M. J.; Jeremic, D.; Hunter, B. K.; Baird, M. C. *Organometallics* **1996**, *15*, 693–703.
- (13) Baxter, S. M.; Ferguson, G. S.; Wolczanski, P. T. *J. Am. Chem. Soc.* **1988**, *110*, 4231–4241.
- (14) Antiñolo, A.; Carrillo-Hermosilla, F.; Corrochano, A.; Fernandez-Baeza, J.; Lara-Sanchez, A.; Ribeiro, M. R.; Lanfranchi, M.; Otero, A.; Pellinghelli, M. A.; Portela, M. F.; Santos, J. V. *Organometallics* **2000**, *19*, 2837–2843.

- (15) Toscano, P. J.; Marks, T. J. *Langmuir* **1986**, *2*, 820–823.
- (16) Morrow, B. A.; Devi, A. *Chem. Commun.* **1971**, 1237–1238.
- (17) Morrow, B. A.; Devi, A. *J. Chem. Soc., Faraday Trans. 1* **1972**, *68*, 403–422.
- (18) Bartram, M. E.; Michalske, T. A.; Rogers, J. W. *J. Phys. Chem.* **1991**, *95*, 4453–4463.
- (19) Scott, S. L.; Basset, J.-M. *J. Am. Chem. Soc.* **1994**, *116*, 12069–12070.
- (20) Morrow, B. A.; Cody, I. A. *J. Phys. Chem.* **1976**, *18*, 2761–2767.
- (21) Morrow, B. A.; Cody, I. A. *J. Phys. Chem.* **1976**, *18*, 1998–2004.
- (22) Nicholas, C. P.; Ahn, H.; Marks, T. J. *J. Am. Chem. Soc.* **2003**, *125*, 4325–4331.

Scheme 1. Comparison of the Grafted Species Obtained on Silica₍₅₀₀₎ and Silica₍₈₀₀₎

local environments. One, **3a** in which a siloxane bridge [$\equiv\text{Si}-\text{O}-\text{Si}\equiv$] is close to the Zr center, depicted as [$(\equiv\text{SiO})\text{ZrCp}^*(\text{Me})_2[\equiv\text{Si}-\text{O}-\text{Si}\equiv]$]. Another one, **3b**, in which, due to the transfer of a methyl group to the surface, highly strained and reactive [$\equiv\text{Si}-\text{O}-\text{Si}\equiv$] bridges of [$\equiv\text{Si}-\text{Me}$] are close to the Zr center.



II. Reactivity of **3a and **3b** with $\text{B}(\text{C}_6\text{F}_5)_3$.** To generate electronically and coordinatively unsaturated cationic alkylzirconium centers,^{23,24} homogeneously dispersed on a silica surface and potentially active in olefin polymerization catalysis,² the reaction of $\text{B}(\text{C}_6\text{F}_5)_3$, with the neutral surface precursor, **3**, was investigated.

II.1. Analytical Data. Impregnation of the white solid **3**, with a slight excess (1.1 equiv) of $\text{B}(\text{C}_6\text{F}_5)_3$ in pentane/toluene 95/5 solution for 3 h at ambient temperature, was followed by the removal of unreacted starting materials. Washing the solid with the same solvents afforded a pale yellow solid **4**. Elemental analysis indicated a percentage of zirconium of 2.2 wt %; (0.81 Zr/nm²) similar to those of the starting complex **3**. There is no detectable leaching of zirconium during the reaction. No significant quantity of methane and pentamethylcyclopentadiene was observed in the gas phase. Unexpectedly hydrolysis of **4** gave 0.6 mol of methane per zirconium instead of 1 mol.

II.2. Spectroscopic Data. The IR spectra of the pale yellow pellets **4**, obtained after impregnation of **3** with a small excess of $\text{B}(\text{C}_6\text{F}_5)_3$ in toluene, exhibited all the bands attributed to

$\nu(\text{C}=\text{C})$ vibrations of the C_6F_5 rings, Figure 1d.^{25–28} In the 3000–2700 cm^{-1} region, the pattern of the $\nu(\text{C}-\text{H})$ absorptions due to methyl groups bound respectively to zirconium and Cp^* ligand was modified after reaction of **3** with $\text{B}(\text{C}_6\text{F}_5)_3$. One should note that the bands attributed to methyl groups present on the Cp^* ligand obscured the $\nu(\text{C}-\text{H})$ vibrations of zirconium methyl groups. To solve this problem, [$(\equiv\text{SiO})\text{ZrCp}^*(\text{CD}_3)_2$] was prepared, **3D**. As already mentioned the $\nu(\text{C}-\text{D})$ and $2\delta(\text{C}-\text{D})$ vibrations of $\text{Zr}-\text{CD}_3$ appear at 2193, 2175, 2077, and 2021 cm^{-1} . After reaction of **3D** with $\text{B}(\text{C}_6\text{F}_5)_3$, the $\nu(\text{C}-\text{D})$ vibrations were shifted at 2225, 2209, and 2136 cm^{-1} . As expected, the bands ascribed to $\nu(\text{C}-\text{H})$ vibrations of Cp^* methyl groups in the 3000–2700 cm^{-1} region for complexes **3D** and **4D** were unaffected, Figure 1e. By subtracting the IR spectrum of the deuterated surface complex **4D** from that of **4**, it is possible to assign the bands corresponding to $\nu(\text{C}-\text{H})$ and $2\delta(\text{C}-\text{H})$ vibrations of the $\text{Zr}-\text{Me}$ groups at 2969, 2936, 2921, and 2879 cm^{-1} of **4** which were also shifted as compared to the vibrations of the methyl groups in **3** (2932, 2911, 2852, and 2757 cm^{-1}). In the 1500–1300 cm^{-1} region, $\nu(\text{C}=\text{C})$ and $\delta(\text{C}-\text{H})$ vibrations of Cp^* ligand and methyl groups are hidden by the strong absorptions of C_6F_5 ligands.

The solid state ¹H NMR spectra of **4** showed only a strong peak at 1.8 ppm characteristic of the methyl groups of the Cp^* ligand, Figure 4. A small shoulder was observed between 0 and 1 ppm, but the signals were not sufficiently well-resolved to be unambiguously ascribed to $\text{Zr}-\text{Me}$ or $\text{B}-\text{Me}$ groups. In the solid state ¹¹B NMR spectra, Figure 5b, a single peak at –18 ppm was present, characteristic of the tetrahedral anionic boron center [$(\text{Me})\text{B}(\text{C}_6\text{F}_5)_3$][–].^{23, 24, 29}

(25) Massey, A. G.; Park, A. J. *J. Organomet. Chem.* **1964**, *2*, 245–250.(26) Chambers, R. D.; Chivers, T. *J. Chem. Soc.* **1964**, 4782–4790.(27) Chambers, R. D.; Chivers, T. *Organomet. Chem. Rev.* **1966**, *1*, 279–304.(28) Bergquist, C.; Bridgewater, B. M.; Harlan, C. J.; Norton, J. R.; Friesner, R. A.; Parkin, G. *J. Am. Chem. Soc.* **2000**, *122*, 10581–10590.(23) Yang, X.; Marks, T. J. *J. Am. Chem. Soc.* **1991**, *113*, 3623–3625.(24) Yang, X.; Stern, C. L.; Marks, T. J. *J. Am. Chem. Soc.* **1994**, *116*, 10015–10031.

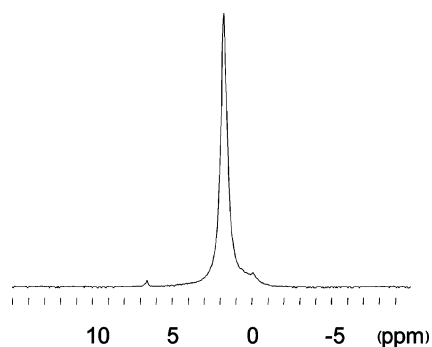


Figure 4. 300 MHz solid state ^1H MAS NMR spectrum of **5***; $[(\equiv\text{SiO})_2\text{ZrCp}^*]^+[(^{13}\text{CH}_3)\text{B}(\text{C}_6\text{F}_5)_3]^-$ spinning speed 10 kHz, recycle delay 2 s.

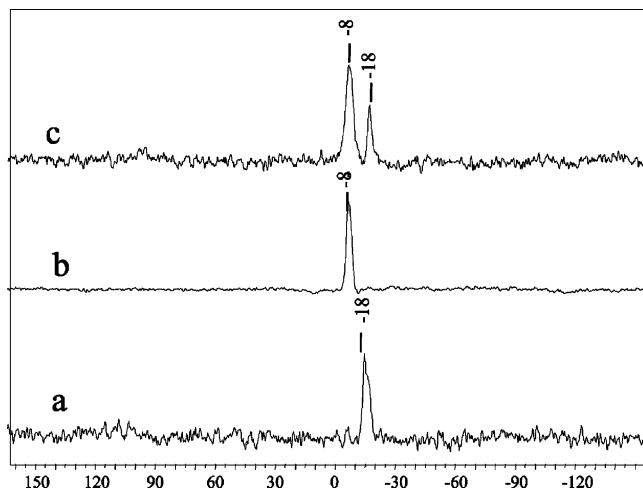


Figure 5. 96 MHz solid state ^{11}B MAS NMR spectra of (a) **4** and **5**; (b) **7**; (c) **9**; spinning speed 10 kHz, recycle delay 1 s.

Solid state ^{13}C NMR spectra of nonlabeled **4** displayed peaks at 125, 129 ppm for the Cp* ligand, suggesting two different species or chemical environments. The peak at 11 ppm is due to the methyl groups of the Cp*, Figure 6a. The carbons of Zr–Me, B–Me, and $[\equiv\text{Si}-\text{Me}]$ groups could not be resolved on these spectra. In the ^{13}C NMR spectrum of $[(\equiv\text{SiO})\text{ZrCp}^*(^{13}\text{CH}_3)_2]$, **3***, Figure 6b, two signals attributed to Zr–Me and $[\equiv\text{Si}-\text{Me}]$ groups were present at 39 and -4.5 ppm, respectively (vide supra). After reaction with $\text{B}(\text{C}_6\text{F}_5)_3$, the peak at 39 ppm was shifted to 55 ppm, as expected for a methyl group bound to a cationic zirconium center, as in a well-characterized homogeneous analogue, for example, $\text{Cp}'_2\text{Zr}^{13}\text{CH}_3^+ \text{CH}_3\text{B}(\text{C}_6\text{F}_5)_3^-$.²⁴

Interestingly the intensity of the signal at -4.5 ppm increased significantly, suggesting that some Me groups were transferred to an adjacent silicon atom, Figure 6c. Simultaneously, two new peaks appeared at 8.3 and 11 ppm, assigned to the methyl group of $[\text{MeB}(\text{C}_6\text{F}_5)_3]$, in two different chemical environments.^{12,23,30,31}

Since the presence of two Cp resonances in the ^{13}C spectra of **4** has been evidenced by NMR, we have performed two types of experiments: one was the hydrolysis, and the other one, the hydrogenolysis of **4**. Hydrolysis of **4** resulted in the disappear-

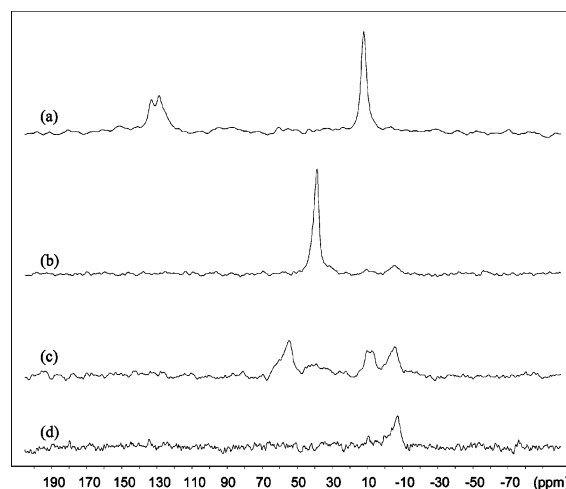


Figure 6. 75 MHz solid state CP MAS ^{13}C NMR of (a) $[(\equiv\text{SiO})\text{ZrCp}^*(\text{Me})_2] + \text{B}(\text{C}_6\text{F}_5)_3$; (b) $(\equiv\text{SiO})\text{ZrCp}^*(^{13}\text{CH}_3)_2$; (c) $[(\equiv\text{SiO})\text{ZrCp}^*(^{13}\text{CH}_3)_2] + \text{B}(\text{C}_6\text{F}_5)_3$; (d) $[(\equiv\text{SiO})\text{ZrCp}^*(^{13}\text{CH}_3)_2] + \text{B}(\text{C}_6\text{F}_5)_3$ after hydrolysis; spinning speed 10 kHz, recycle delay 2 s, contact time 5 ms.

ance of all the peaks (at 55, 11, and 8.3 ppm ascribed to Zr–Me and B–Me) except the one corresponding to the $[\equiv\text{Si}-\text{Me}]$ group at -4.5 ppm (Figure 6d). Hydrolysis also resulted in the evolution of only 0.6 equiv of methane/Zr instead of 2 equiv expected for $[(\equiv\text{SiO}_{800})\text{ZrCp}^*(\text{Me})]^+[(\text{Me})\text{B}(\text{C}_6\text{F}_5)_3]^-$ (1 equiv for the Zr–Me bond and 1 equiv for the B–Me bond); hydrogenolysis of **4**, or **4***, gave 0.3 mol of methane/Zr instead of 1 mol for $[(\equiv\text{SiO}_{800})\text{ZrCp}^*(\text{Me})]^+[(\text{Me})\text{B}(\text{C}_6\text{F}_5)_3]^-$ (for one Zr–Me bond).

These results indicate that only ca. 30% of the zirconium corresponds effectively to the expected structure $[(\equiv\text{SiO}_{800})\text{ZrCp}^*\text{Me}]^+[(\text{Me})\text{B}(\text{C}_6\text{F}_5)_3]^-$. Unexpectedly 70% of the surface zirconium complex has no methyl ligands!

II.3. Conclusions. The data can be interpreted by the coexistence of three different species that we shall call **4a**, **4b**, and **5**. These structures are derived from the known structures of **3a** and **3b**, Scheme 2. **4a** and **4b** present the same “designed” and “expected” cationic structure but in two different environments: $[\equiv\text{Si}-\text{O}-\text{Si}\equiv]$ and $[\equiv\text{Si}-\text{Me}]$ functionalities. Unfortunately for the catalytic purpose, these are minor species. The most abundant species is the bipodal **5** which results from the transformation of the starting monopodal complex **4a** by transfer of one methyl from the Zr to the surface. This occurs by opening of $[\equiv\text{Si}-\text{O}-\text{Si}\equiv]$ bridges. The resulting species **5** does not bear any methyl group. We propose that the methyl transfer to the surface is due to the highly electrophilic and oxophilic character of the cationic zirconium. EXAFS data obtained on similar systems have suggested the presence, in the coordination sphere of hafnium and tantalum, an oxygen atom at 2.706 and 3.024 Å, respectively, which can be assigned to a siloxane bridge acting as a two-electron donor ligand to stabilize the otherwise highly electron deficient surface complex. The oxophilicity of zirconium favors the cleavage of the $[\equiv\text{Si}-\text{O}-\text{Si}\equiv]$ bond and concomitant formation of a new $\equiv\text{Si}-\text{O}-\text{Zr}$ and $\equiv\text{Si}-\text{Me}$ bonds. Consequently, **5** is the major (70%) surface species.

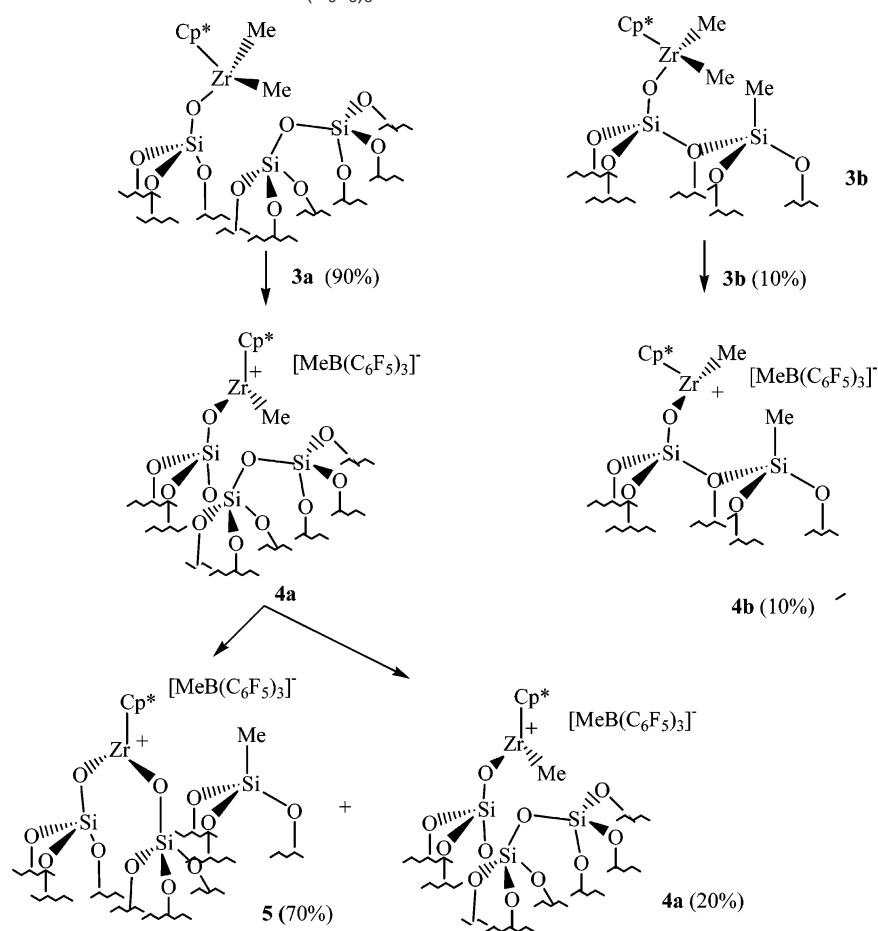
These results clearly show that this route does not afford single site heterogeneous catalysis. Similar reaction pathways were reported for molecular analogues.³² Only 30% of **3**

(29) Hill, G. S.; Manojlovic-Muir, L.; Muir, K. W.; Puddephatt, R. J. *Organometallics* **1997**, *16*, 525–530.

(30) Gillis, D. J.; Tudoret, M. J.; Baird, M. C. *J. Am. Chem. Soc.* **1993**, *115*, 2543–2545.

(31) Thorn, M. G.; Etheridge, Z. C.; Fanwick, P. E.; Rothwell, I. P. *J. Organomet. Chem.* **1999**, *591*, 148–162.

(32) Metcalfe, R. A.; Kreller, D. I.; Tian, J.; Kim, H.; Taylor, N. J.; Corrigan, J. F.; Collins, S. *Organometallics* **2002**, *21*, 1719–1726.

Scheme 2. Grafted Species Formed after Addition of $B(C_6F_5)_3$ on **3a** and **3b**

was converted to the designed catalyst $[(\equiv SiO)ZrCp^*(Me)]^+ [MeB(C_6F_5)_3]^-$, **4**.

III. Reactivity of Cp^*ZrMe_3 with $[(\equiv SiO)B(C_6F_5)_3]^- [HNEt_2Ph]^+$. It has been previously shown that the reaction of tris(pentafluorophenyl)boron, $B(C_6F_5)_3$, with surface silanol ($\equiv Si-OH$) of silica occurs *only* in the presence of Brønsted base diethylaniline, Et_2NPh , which does not form a complex with $B(C_6F_5)_3$, and affords selectively a well-defined ionic entity $[(\equiv SiO)B(C_6F_5)_3]^- [HNEt_2Ph]^+$.^{5,6,8,9} Without a base $B(C_6F_5)_3$ does not react with ($\equiv Si-OH$) and is only physisorbed. The interaction of $B(C_6F_5)_3$ with silica in the presence of Et_2NPh yields $[(\equiv Si-O)B(C_6F_5)_3]^- [HNEt_2Ph]^+$, **6**.^{33,34}

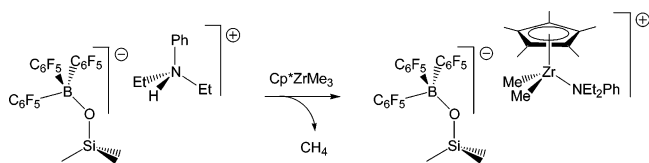
Recently we have reported that the reaction of the well-defined heterogeneous activator $[(\equiv SiO)B(C_6F_5)_3]^- [HNEt_2Ph]^+$, **6**, with $Cp^*Zr(Me)_3$, affords the unique and fully characterized surface species $[(\equiv SiO)B(C_6F_5)_3]^- [Cp^*Zr(Me)_2(NEt_2Ph)]^+$, **7**, in which the surface is indeed a noncoordinating anion.⁸

Typically, the preparation of **7** was achieved by stirring for 1 h at 25 °C a mixture of 1.50 g of **6** (0.31 mmol of surface anilinium) with 102 mg of $Cp^*Zr(Me)_3$ (0.38 mmol) in pentane and led to the evolution of 0.36 mmol of methane as the only gaseous product detected. This corresponds to 1.1 ± 0.1 methane formed/initial available surface fragments $[(\equiv SiO)B(C_6F_5)_3]^- [HNEt_2Ph]^+$. The resulting pale yellow surface organometallic species **7**, obtained after washing the excess of $Cp^*Zr(Me)_3$ and drying under a high vacuum at 25 °C, contains 1.77 wt % of Zr (0.64 Zr/nm²). This elemental analysis is in agreement with the grafting of one Zr per initial surface

fragments $[(\equiv SiO)B(C_6F_5)_3]^- [HNEt_2Ph]^+$ available on **6**. These numbers are further confirmed by the hydrolysis of **7** at 25 °C which produces 1.97 ± 0.2 equiv of methane per Zr. No pentamethylcyclopentadiene is detected in the impregnation filtrates or in pentane extracts. Therefore, the surface complex **7** is a zirconium complex monografted to the modified silica surface **6** and surrounded by two methyl and one pentamethylcyclopentadienyl ligands. Infrared studies confirm that $Cp^*Zr(Me)_3$ reacts primarily with the surface anilinium cation as shown by the disappearance of the $\nu(N-H)$ vibration at 3232 cm^{-1} initially present in the spectrum of **6**. Activation of neutral metallocenes via irreversible protonolysis reaction with ammonium cations has been reported for molecular analogues.⁹ Simultaneously, new bands characteristic of alkyl groups appear at 2983, 2957, and 2740 cm^{-1} . Moreover, IR spectra of surface complex **7D** obtained by reaction of $Cp^*Zr(CD_3)_3$, with **6**, exhibit bands at 2199, 2133, 2091, 2038 cm^{-1} ascribed to $Zr-CD_3$ fragments, which unambiguously attests to the subsistence of surface $Zr-Me$ groups on **7** after the grafting step.⁵

Solid-state CP-MAS ¹³C NMR spectra of **7** give two signals at 9 and 42 ppm attributed to methyl groups bound to the Cp^* ligand and zirconium atom, respectively. The peak at 42 ppm whose intensity strongly increased for the ¹³C labeled enriched species **7*** (99% labeled), is characteristic of a cationic $Zr-^{13}CH_3$ moiety.²³ Additionally, the second peak ($\delta = 9$ ppm) present in **7*** can be independently attributed to the Cp^* ligand or to the free $[(^{13}CH_3)B(C_6F_5)_3]^-$ anion. ¹H-¹³C HETCOR solid state NMR experiments permit us to unambiguously assign the

latter peak to methyl groups of the Cp* ligand. The existence of surface Zr—¹³CH₃ groups is also confirmed after hydrolysis of **7*** leading to the complete disappearance of the resonance at 42 ppm. Only peaks representative of the ring carbons (120 ppm) and methyl groups (9 ppm) of the Cp* ligand are still present on **7*** after hydrolysis. The fact that nearly 2 equiv of methane per zirconium are liberated after hydrolysis, combined with the ¹³C NMR spectra recorded for **7*** after hydrolysis, also supports the presence of a surface [Cp*Zr(Me)₂]⁺ fragment. Solid state ¹¹B NMR spectra of **7**, Figure 5, display a strong and sharp resonance at -8 ppm indicating that the surface anion [(≡SiO)B(C₆F₅)₃]⁻ is still present after reaction of Cp*Zr(Me)₃ with **6**. However, all the data indicate that the aniline ligand remains in the coordination sphere of the zirconium.

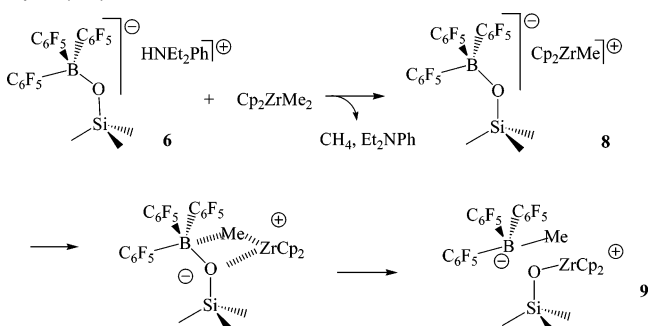


IV. Reactivity of Cp₂Zr(Me)₂ with [(≡SiO)B(C₆F₅)₃]⁻[HNEt₂Ph]⁺. The fact that the aniline ligand remains coordinated could be due to an insufficient steric hindrance in the cationic moieties [Cp*Zr(Me)₂]⁺. With (η⁵-C₅H₅)₂Zr(Me)₂ as starting material, the presence of two Cp groups increases both the steric hindrance in the coordination sphere of zirconium and the electronic density on the zirconium atom, therefore hindering the coordination of NEt₂Ph.

IV.1.1. Analytical Data. The reaction of Cp₂Zr(Me)₂ [124 mg, 0.49 mmol] with **6** [2 g, 0.31 mmol of surface anilinium] was achieved in pentane, 2 h at 20 °C, and led to the evolution of 0.48 mmol of methane as the only gaseous product detected. The resulting pale yellow surface species **8** was obtained after washing the excess of Cp₂Zr(Me)₂ and drying under a high vacuum at 25 °C. Elemental analysis showed 1.07 B/grafted Zr and 27 C/grafted Zr (Th. 29 for 2Cp 1Zr 1Me and 3C₆F₅) (0.23, 2.09, and 7.34 w % of B, Zr, and C, respectively) and the ratio N/grafted Zr being close to 0. The elemental analysis was in agreement with the elimination of 1.07 equiv of methane/Zr during the grafting process and the grafting of one Zr per initial surface fragment [(≡SiO)B(C₆F₅)₃]⁻[HNEt₂Ph]⁺ available on **6** and with a complete elimination of aniline. No cyclopentadiene was detected in the impregnation filtrates or in pentane extracts.

IV.1.2. Spectroscopic Data. Solid state ¹H NMR spectra of **8** exhibited two peaks at 7 and 0.7 ppm ascribed, respectively, to the protons of the Cp ligand and to a methyl group bonded either to a zirconium atom or to boron. In accordance with elemental analysis, no peak due to NEt₂Ph was detected supporting the fact that NEt₂Ph had been eliminated upon grafting. The CP-MAS ¹³C NMR spectra of **8** showed only one peak at 115 ppm attributed to the Cp ligand. The CP-MAS ¹³C NMR spectra of **8*** (using Cp₂Zr(¹³CH₃)₂) exhibited one peak at 11 ppm. The species responsible for this peak is slowly eliminated under water atmosphere, which strongly suggests that it is not a Zr—Me group (we shall see later that a water sensitive transient peak at 22 ppm is quickly transformed under vacuum into the peak at 11 ppm). This hypothesis is corroborated by the fact that for the cationic Zr—¹³CH₃ moiety the resonances are expected at δ = 46 ppm and NDR 0.46 ppm),^{9,22,30,35} and

Scheme 3. Grafted Species Formed during the Addition of Cp₂Zr(Me)₂ on **6**



for neutral Zr—Me the resonances are expected at δ = 22 ppm.^{7,22} The solid state ¹¹B NMR spectra of **8** displayed two strong and sharp resonances, one at -8 ppm and the other at -17 ppm indicating the simultaneous presence of the surface anions [(≡SiO)B(C₆F₅)₃]⁻^{8,9} and [MeB(C₆F₅)₃]⁻, Figure 5c.^{23,24,29,36} The presence of a methyl group linked to the boron atom suggests there is a metathetical exchange between B—O—Si and Zr—Me, due to the higher oxophilicity of the zirconium atom in [Cp₂Zr(Me)]⁺ compared to that of the boron atom in [(≡SiO)B(C₆F₅)₃]⁻.

To summarize the results, the interaction between Cp₂Zr(Me)₂ and [(≡SiO)B(C₆F₅)₃]⁻[HNEt₂Ph]⁺ leads to a thermodynamically stable product [(≡SiO)ZrCp₂]⁺[(Me)B(C₆F₅)₃]⁻, **9**.

All the spectroscopic and analytical data are supporting this final undesired structure.

The looked-for structure **8** [(≡SiO)B(C₆F₅)₃]⁻[Cp₂Zr(Me)]⁺ is not observed. The intermediate showing a resonance at 22 ppm can correspond either to the neutral surface complex [≡Si—O—ZrMeCp₂] or to a bimolecular surface complex with a bridged methyl group between the atoms of boron and zirconium [(≡SiO)B(C₆F₅)₃...Me...ZrCp₂]⁺.² Finally these transient complexes are transformed into **9**.

These successive steps affording a stable and probably inactive complex have also been established with the molecular analogues derived from silsesquioxanes³² and by a DRIFTS study for silica-supported zirconocene perfluorophenylborate catalyst.³⁷

V. Catalytic Polymerization of Ethylene. The objective of this work was to compare the catalytic activity of cationic zirconium complexes covalently bonded to a silica surface, such as [(≡SiO)ZrCp*(Me)]⁺[(Me)B(C₆F₅)₃]⁻, **4**, with “floating” cationic zirconium complexes such as [≡Si—C⁺R]⁻[MR_{n-1}]⁺. Unfortunately we have shown that it was impossible to stabilize, at least in our conditions, such a complex. Instead we have been able to prepare [(≡SiO)B(C₆F₅)₃]⁻[Cp*Zr(Me)₂·NEt₂Ph]⁺, **7**.

Only two “relatively well-defined” compounds grafted on SiO₂-(800), [(≡SiO)ZrCp*Me]⁺[(Me)B(C₆F₅)₃]⁻, **4**, and [(≡SiO)B(C₆F₅)₃]⁻[Cp*Zr(Me)₂·NEt₂Ph]⁺, **7**, could be tested in ethylene

(33) Millot, N.; Santini, C. C.; Fenet, B.; Basset, J.-M. *Eur. J. Inorg. Chem.* **2002**, 3328–3335.

(34) Millot, N.; Santini, C. C.; Lefebvre, F.; Basset, J.-M. *C. R. Chimie* **2004**, *7*, 725–736.

(35) Gillis, D. J.; Quyoum, R.; Tudoret, M. J.; Wang, Q.; Jeremic, D.; Roszak, A. W.; Baird, M. C. *Organometallics* **1996**, *15*, 3600–3605.

(36) Siedle, A. R.; Newmark, R. A.; Lamanna, W. M.; Huffman, J. C. *Organometallics* **1993**, *12*, 1491–1492.

(37) Panchenko, V. N.; Danilova, I. G.; Zakharov, V. A.; Paukshitis, E. A. *J. Mol. Catal. A* **2005**, *225*, 271–277.

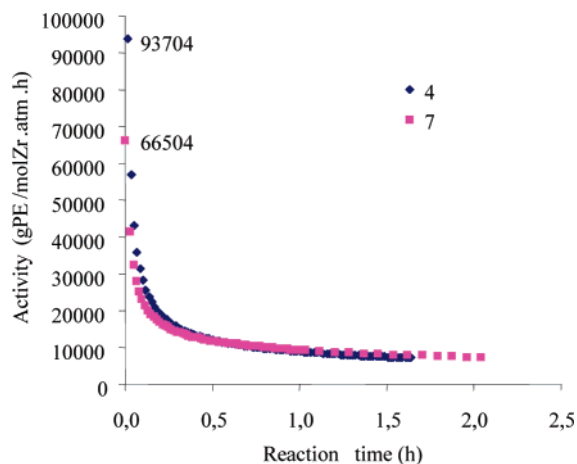


Figure 7. Infrared monitoring of ethylene polymerization activity with reaction time for **4** and **7** (25 °C, ca. 100 mg of solid catalyst 200 Torr of dry ethylene at initial time, t_0).

polymerization. Their intrinsic catalytic activities, without cocatalyst, have been monitored by IR spectroscopy of the gas phase.

V.1. Initial Activity by IR Spectroscopy. The activity of **4** and **7** toward ethylene polymerization catalysis was first qualitatively studied by following the appearance of polyethylene vibrations on silica pellets. The latter were exposed to ethylene pressure (200 Torr) and introduced into the infrared cell at ambient temperature, for 4 h. After exposure of **4** and **7** to ethylene, intense bands appeared at 2970, 2850, and 1380 cm^{-1} corresponding, respectively, to $\nu(\text{C}-\text{H})$ and $\delta(\text{C}-\text{H})$ vibrations of polyethylene. These results confirm that both **4** and **7** were active catalysts for ethylene polymerization.

V.2. Rate of Ethylene Polymerization. The initial rates of **4** and **7** toward ethylene polymerization were qualitatively evaluated by measuring the disappearance of the monomer in the gas phase in infrared spectroscopy. The solid catalysts (100 mg) were placed in a closed glass tube connected to a high vacuum infrared cell via a break-seal. The disappearance of ethylene was monitored through the integration of the entire $\nu(\text{C}-\text{H})$ spectral region (3300–2700 cm^{-1}) of the gas phase. The reactions were performed at room temperature under a low pressure (200 Torr) of dry ethylene (note that the ethylene pressure was not maintained constantly during the course of the reaction). The initial time, t_0 , was determined when the sealed reactor containing the catalyst was broken. Several experiments were carried out in these conditions with the catalysts **4** and **7** on $\text{SiO}_{2-(800)}$ at various zirconium loadings; the maximum activities are reported in Figure 7.

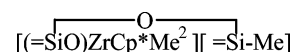
For both catalysts, fast deactivation was observed with time (activities were halved after 3 min). Several factors might explain this phenomenon: decrease of the concentration of ethylene in the gas phase as the polymerization proceeds, inaccessibility of the active sites covered by the resulting polyethylene and/or unfavorable mass transfer of ethylene to the active site in our conditions. The introduction of an additional pressure of ethylene at the end of a catalytic test for **7** (not performed on **4**) led to the continuous consumption of the monomer, thus showing that active sites were still present in the system.

Previous results obtained in the laboratory concerning similar systems grafted on alumina pretreated at 500 and 1000 °C are

depicted in Table 1.⁷ Comparison of the activities of our silica supported cationic systems with the previously prepared alumina one, Table 1, measured under strictly identical experimental conditions, shows that **4** and **7** seem the most efficient systems. If one considers that in **4** only 30% of zirconium keeps its methyl group (70% of **4a** gives spontaneously **5** *vide supra*) (see Scheme 2), **4** presents the highest intrinsic activity. However, further studies on these catalytic systems to confirm this result are currently under study.

Conclusion

The reaction of Cp^*ZrMe_3 with $\text{SiO}_{2-(800)}$ affords a well-defined surface species $[(\equiv\text{SiO})\text{ZrCp}^*(\text{Me})_2]$, **3**, but with two different local environments: **3a** $[(\equiv\text{SiO})\text{ZrCp}^*\text{Me}_2][\equiv\text{Si}-\text{O}-\text{Si}\equiv]$ and the other with **3b**,



through two pathways, (a) protolysis of a Zr-Me group by surface silanols and (b) transfer of a methyl group to the surface by opening siloxane groups, with a relative proportion of ca. 9/1, respectively.

The reaction of **3** with $\text{B}(\text{C}_6\text{F}_5)_3$ is controlled by these local environments. $[(\equiv\text{SiO})\text{ZrCp}^*(\text{Me})]^+[(\text{Me})\text{B}(\text{C}_6\text{F}_5)_3]^-$, **4**, is in two different environments: one with $[\equiv\text{Si}-\text{O}-\text{Si}\equiv]$ groups, **4a**, and the other with $[\equiv\text{Si}-\text{Me}]$, **4b**. Unfortunately these are minor species (30%). The most abundant species is the bipodal $[(\equiv\text{SiO})_2\text{ZrCp}^*]^+[(\text{Me})\text{B}(\text{C}_6\text{F}_5)_3]^-$, **5** (70%), resulting from the transformation of **4a** by transfer of one methyl from the Zr to the surface through the opening of $[\equiv\text{Si}-\text{O}-\text{Si}\equiv]$ bridges.

The reactions $\text{Cp}^*\text{Zr}(\text{Me})_3$ and of $\text{Cp}_2\text{Zr}(\text{Me})_2$ with $[(\equiv\text{SiO})\text{B}(\text{C}_6\text{F}_5)_3]^-[\text{HNEt}_2\text{Ph}]^+$ afford $[(\equiv\text{SiO})\text{B}(\text{C}_6\text{F}_5)_3]^-[\text{Cp}^*\text{Zr}(\text{Me})_2\cdot\text{NEt}_2\text{Ph}]^+$, **7**, and $[(\equiv\text{SiO})\text{ZrCp}_2]^+[(\text{Me})\text{B}(\text{C}_6\text{F}_5)_3]^-$, **9**, respectively. **9** results from a metathetical exchange between $\text{B}-\text{O}-\text{Si}$ and $\text{Zr}-\text{Me}$, due to the higher oxophilicity of zirconium in $[\text{Cp}_2\text{Zr}(\text{Me})]^+$ compared to that of B in $[(\equiv\text{SiO})\text{B}(\text{C}_6\text{F}_5)_3]^-$.

All complexes have been fully characterized by elemental and gas phase analyses, spectroscopic methods (infrared, multinuclear solid state NMR), and isotopic labeling (^2H , ^{13}C).

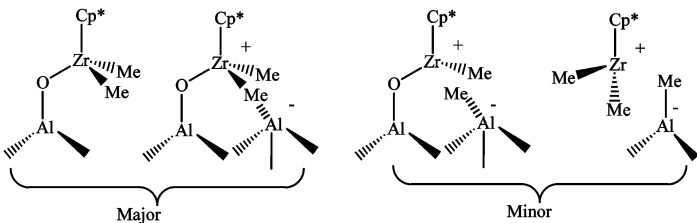
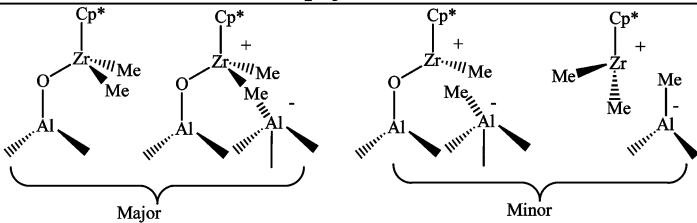
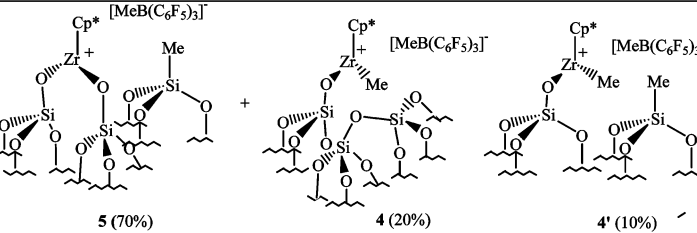
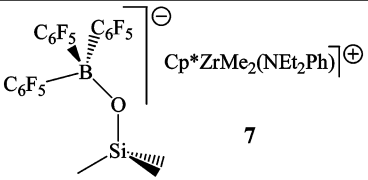
$[(\equiv\text{SiO})\text{ZrCp}^*(\text{Me})]^+[(\text{Me})\text{B}(\text{C}_6\text{F}_5)_3]^-$, **4**, and $[(\equiv\text{SiO})\text{B}(\text{C}_6\text{F}_5)_3]^-[\text{Cp}^*\text{Zr}(\text{Me})_2\cdot\text{Et}_2\text{NPh}]^+$, **7**, are active catalysts toward ethylene polymerization at ambient temperature. Rapid deactivation of the catalytic systems is observed; **4** exhibits the highest intrinsic activity.

These results can be a first step in the comprehension of the deactivation of supported cationic zirconium in the catalytic polymerization of olefins with supported metallocenes. There is successive opening of the siloxane bridge with concomitant formation of $[\equiv\text{Si}-\text{Me}]$ and of a supplementary bond $[\equiv\text{Si}-\text{O}-\text{Zr}]$. Consequently, the Zr atom is “stripped” of its Me groups and progressively buried into the oxide surface. Current research is directed toward preventing this deactivation using either a partially modified silica with a $[\equiv\text{Si}-\text{R}]$ bond or a second alkylating cocatalyst to regenerate a metal-alkyl bond from a $[\equiv\text{Si}-\text{O}-\text{Zr}]$ bond.

Experimental Section

MAS and CPMAS solid-state NMR spectra were recorded on a Bruker DSX-300 spectrometer equipped with a standard 4 mm probe head and operating at 75.47, 96.31, and 300.18 MHz for ^{13}C ,

Table 1. Comparison of the Maximum Activity for **4**, **7**, and Supported Analogues^a

Catalysts	% Zr	Activity [c]
 <p style="text-align: center;">Major Minor</p> <p style="text-align: center;">Al₂O₃-500°C</p>	1.8	13
 <p style="text-align: center;">Major Minor</p> <p style="text-align: center;">Al₂O₃-1000°C</p>	1.4	20
 <p style="text-align: center;">5 (70%) 4 (20%) 4' (10%)</p>	2.2	93
 <p style="text-align: center;">7</p>	1.7	67

^a Experimental conditions: $P_{C_2H_4} = 200$ Torr; $V_{\text{reactor}} = 320$ mL; $n_{C_2H_4}/n_{Zr} = 170$; $m_{\text{catal.}} = 100$ mg.

¹¹B, and ¹H, respectively. Chemical shifts are given relative to external references (¹H, ¹³C, TMS at 0; ¹¹B, BF₃·OEt₂ at 0). The samples were packed in the zirconia rotor in a glovebox and tightly closed. Infrared spectra were recorded under a vacuum on a Nicolet 550 FT spectrometer by using an infrared cell equipped with CaF₂ windows. Typically 16 scans were accumulated for each spectrum. Elemental analyses were performed by the Central Analysis Service of the CNRS at Solaise.

All operations were performed in the strict absence of oxygen and water under a purified argon atmosphere using glovebox (Jacomex or MBraun) or vacuum-line techniques. Toluene and pentane were distilled from a Na/K alloy, degassed, and stored under argon over Na (toluene) or 3 Å molecular sieves (pentane). Ether was distilled under nitrogen from sodium benzophenone ketyl and used immediately. NEt₂Ph (Aldrich Chemicals, 98%) was dried over KOH, distilled under vacuum, and used immediately. B(C₆F₅)₃ (Merck Chemicals, > 97%) was dried on MeSiCl₃ purified by vacuum sublimation, and the purity is checked by ¹⁹F NMR before use. Cp*ZrCl₃ (99%) and Cp₂ZrCl₂ were purchased from Strem Chemicals; MeMgI, ¹³CH₃I (99%), and CD₃MgI (>99%) were purchased from Aldrich Chemicals and used without further purification. ¹³CH₃MgI Cp*ZrMe₃⁴⁰ and Cp₂ZrMe₂⁴¹ were prepared according to literature procedures. CD₃MgI and ¹³CH₃MgI were used for the preparation of the labeled compounds Cp*Zr(CD₃)₃, Cp*Zr-(¹³CH₃)₃, and Cp₂Zr(¹³CH₃)₂. Silica support (Aerosil Degussa, 200 m²/g) was pretreated at 400 °C in air for 4 h and dehydroxylated at 800 °C under a high vacuum (10⁻⁵ Torr) for 12 h (referred as SiO₂-(800)).

The surface area measured by N₂ adsorption and treatment of data using a BET method was 180 m²/g for SiO₂-(800). Preparation of **6** and **7** was as previously described.⁸

Synthesis of Silica Surface Complexes [(≡SiO)ZrCp*(Me)₂], **3, [(≡SiO)ZrCp*(CD₃)₂], **3_D**, and [(≡SiO)ZrCp*(¹³CH₃)₂], **3***. Preparation of **3**. General procedure A for infrared experiments:** In a glovebox, a pellet of typically 30 mg of compacted silica, previously dehydroxylated at 800 °C, was impregnated under argon during 3 h at ambient temperature with a solution of 5 equiv of Cp*Zr(Me)₃ (8.5 mg – 0.03 mmol) in 10 mL of dry pentane. The white pellet was then washed with three fractions (10 mL) of dry pentane, introduced in the infrared cell, and dried for 1 h under a high vacuum (10⁻⁵ Torr). IR: 2980 (m, ν_{as}(C–H)Cp*), 2954 (m, ν_{as}(C–H)Cp*), 2920 (m, ν_s(C–H)Cp* and ν_{as}(C–H)Zr–Me), 2869 (m, 2δ_{as}(C–H)Cp* and ν_s(C–H)Zr–Me), 2781 (w), 2767 (w), 2757 (w, 2δ_{as}(C–H)Zr–Me), 2740 (w), 1492 (w, ν(C=C)Cp*), 1459 (w, δ_{as}(C–H)Cp*), 1439 (w, ν(C=C)Cp*), 1392 (w, δ_{as}(C–H)Zr–Me), 1383 (w, δ_s(C–H)Cp* and ν(C=C)Cp*).

General procedure B for larger scale preparation (NMR and elemental analysis samples): In a Schlenk tube, 2 g of SiO₂-(800) were

(38) Lancaster, S. J.; O'Hara, S. M.; Bochmann, M. In *Metalorganic Catalysts for Synthesis and Polymerisation*; Kaminsky, W., Ed.; Springer, 1999.

(39) Hlatky, G. G. *Chem. Rev.* **2000**, *100*, 1347–1376.

(40) Wolczanski, P. T.; Bercaw, J. E. *Organometallics* **1982**, *1*, 793–799.

(41) Wailes, P. C.; Weigold, H.; Bell, A. J. *Organomet. Chem.* **1972**, *34*, 105–164.

impregnated during 3 h at ambient temperature with a solution of 136 mg (0.5 mmol – 1.2 equiv) of Cp^*ZrMe_3 in 10 mL of dry pentane. The impregnation supernatant was then vacuum transferred at 73 K in a large glass flask of known volume (for quantification of the volatile and gaseous products), and the solid was washed 4 times with 15 mL of dry pentane. A white powder was obtained after drying for 1 h under a vacuum (10^{-5} Torr) and at room temperature. Wt % Zr: 1.35%.

Preparation of 3_D. *Procedure A* from $\text{Cp}^*\text{Zr}(\text{CD}_3)_3$ [8.8 mg (0.03 mmol – 5 equiv)] pentane (10 mL). IR: 2981 (m, $\nu_{\text{as}}(\text{C-H})\text{Cp}^*$), 2956 (m, $\nu_{\text{as}}(\text{C-H})\text{Cp}^*$), 2920 (m, $\nu_{\text{s}}(\text{C-H})\text{Cp}^*$), 2870 (m, $2\delta_{\text{as}}(\text{C-H})\text{Cp}^*$), 2819 (w), 2782 (vw), 2769 (vw), 2749 (vw), 2739 (w), 2225 (vw), 2193 (w, $\nu_{\text{as}}(\text{C-D})\text{Zr-CD}_3$), 2175 (w, $\nu_{\text{as}}(\text{C-D})\text{Zr-CD}_3$), 2137 (vw), 2077 (w, $\nu_{\text{s}}(\text{C-D})\text{Zr-CD}_3$), 2021 (vw, $2\delta_{\text{as}}(\text{C-D})\text{Zr-CD}_3$), 1491 (w, $\nu(\text{C=C})\text{Cp}^*$), 1457 (w, $\delta_{\text{as}}(\text{C-H})\text{Cp}^*$), 1437 (w, $\nu(\text{C=C})\text{Cp}^*$), 1429 (w), 1390 (vw, $\nu(\text{C=C})\text{Cp}^*$), 1382 (w, $\delta_{\text{s}}(\text{C-H})\text{Cp}^*$).

Preparation of 3*. *Procedure B* from $\text{Cp}^*\text{Zr}(\text{C}^{13}\text{CH}_3)_3$ [55 mg ($n = 0.2$ mmol – 0.7 equiv)] pentane (10 mL) $\text{SiO}_{2-(800)}$ (1.5 g) pentane (10 mL); white solid; wt % Zr: 1.12–1.08%.

Hydrolysis of Compounds 3 (3*). An excess of water (relative to Zr content) was condensed at 73 K under a vacuum onto 100 mg of 3 (3*). The white solid was then allowed to warm to room temperature. No color change was observed under a vapor pressure of water. Gas phase analysis (GC): 2–2.3 CH_4/Zr . Solid state ^1H NMR (δ): 3 (3*) 1.5–2.1 (s, Me–Cp*), no Zr–Me observed at –0.25 ppm. Solid state ^{13}C NMR (δ): (3*) 122 (s, $\text{C}_{\text{ring}}\text{-Cp}^*$), 11 (s, Cp*–Me), –5.7 (s, Si– $^{13}\text{CH}_3$); (3) 122 (s, $\text{C}_{\text{ring}}\text{-Cp}^*$), 10 (s, Cp*–Me).

Hydrogenolysis of Compounds 3. Under a vacuum at ambient temperature, a pressure of 200–250 Torr (40–50 equiv relative to Zr content) of hydrogen was introduced onto 100 mg of 3. The reactor was then warmed to 75 °C for 15 h. The initially white color of the solid turned to light yellow. Gas phase analysis (GC): 1.6 CH_4/Zr . Solid state ^1H NMR (δ): (3) 9.5 (s, Zr–H), 1.7 (s, Me–Cp*), –0.34 (s, residual Zr–Me). Solid state ^{13}C NMR (δ): (3) 121 (s, $\text{C}_{\text{ring}}\text{-Cp}^*$), 9 (s, Cp*–Me), no Zr–Me observed.

Reaction of Silica Surface Complexes [(SiO)ZrCp*(Me)₂], 3, [(SiO)ZrCp*(CD₃)₂], 3_D, and [(SiO)ZrCp*(¹³CH₃)₂], 3* with B(C₆F₅)₃.
Preparation of 4 and 5. *Procedure A* from a pellet of 3, B(C₆F₅)₃ (16 mg – 0.03 mmol), and toluene (10 mL); IR: 2964 (m, $\nu_{\text{as}}(\text{C-H})\text{Cp}^*$), 2924 (m, $\nu_{\text{s}}(\text{C-H})\text{Cp}^*$ and $\nu_{\text{as}}(\text{C-H})\text{Zr-Me}$), 2873 (m, $2\delta_{\text{as}}(\text{C-H})\text{Cp}^*$ and $\nu_{\text{s}}(\text{C-H})\text{Zr-Me}$), 2741 (w), 1601 (w), 1553 (w), 1483 (w.sh., $\nu(\text{C=C})\text{Cp}^*$), 1432 (m.sh., $\nu(\text{C=C})\text{Cp}^*$), 1391 (w.sh., $\delta_{\text{as}}(\text{C-H})\text{Zr-Me}$ and C₆F₅ groups), 1384 (w, $\delta_{\text{s}}(\text{C-H})\text{Cp}^* - \nu(\text{C=C})\text{Cp}^*$ and C₆F₅ groups), 1337 (m), 1314 (w) – medium to strong absorptions characteristic of two different types of C₆F₅ groups appeared at 1646 (m), 1517 (s, $\nu(\text{C=C})$), 1462 (vs, $\nu(\text{C=C})$), 1391 (m) and 1634 (m), 1507 (s, $\nu(\text{C=C})$), 1449 (vs, $\nu(\text{C=C})$), 1384 (m).

Procedure B from 3 (2 g), B(C₆F₅)₃ [236 mg (0.46 mmol – 1.1 equiv)] pentane or pentane/toluene (95/5) (15 mL), pale yellow powder; wt % Zr: 1.08–1.42%. Solid state ^1H NMR (δ): 6.6 (s, residual aromatic protons of toluene), 1.8 (s, Me–Cp*), –0.1 to –0.3 (s, $\equiv\text{Si-Me}$), Zr–Me, and B–Me not well-resolved.

Hydrolysis of Compounds 4 and 5. The same procedure as that for compound 3. (GC): 0.4–0.5 CH_4/Zr . Solid state ^1H NMR (δ): (5*) 1.6 (s, Me–Cp*). Solid state ^{13}C NMR (δ): (5*) 12 (s, Cp*–Me), –4.5 (s, $\equiv\text{Si-}^{13}\text{CH}_3$), neither Zr–Me nor B–Me observed.

Hydrogenolysis of Compounds 4 and 5. The same procedure as that for compound 3. (GC): 0.27 CH_4/Zr . Solid state ^1H NMR (δ): 6.4 (s, residual toluene), 1.6 (s, Me–Cp*), 0.0 (s, $\equiv\text{Si-Me}$). Solid state ^{13}C NMR (δ): 129.1 (s, $\text{C}_{\text{ring}}\text{-Cp}^*$), 10.7 (s, Cp*–Me).

Preparation of 9. *Procedure B* from 8 [0.49 mmol – 1.2 equiv], 1(2 g), pentane (15 mL); wt % Zr: 1.74–1.81%. Gas phase analysis (GC): 1.01–1.22 CH_4/Zr .

Ethylene Polymerization Tests. Gas Phase Polymerization Runs on Silica Pellets. A known pressure of dry and deoxygenated ethylene (200 Torr, 300 equiv) was introduced on silica pellets of 4 or 7 (30 mg) at ambient temperature. The formation of the polyethylene was followed on the silica disk by infrared spectroscopy during 1 day and at room temperature.

Gas Phase Polymerization Runs on Powder. The catalysts 4 or 7 (100 mg) were placed in a break-seal glass high vacuum reactor connected to an infrared cell. A pressure of dry and deoxygenated ethylene (200 Torr, 190 equiv) was introduced in the cell at ambient temperature, and a spectrum of the gas phase was recorded (t_0). The sealed reactor was then broken, and the consumption of the ethylene was followed by infrared spectroscopy of the gas phase as a function of time at room temperature.

Acknowledgment. We are grateful to the French Ministry for a fellowship (M.N.).

JA060420+